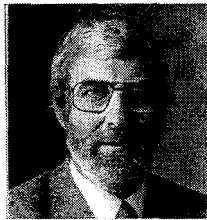


IR SPECTROSCOPY AS A PROBE OF OBSCURED AGN

Alan F. M. Moorwood

European Southern Observatory, D-85748 Garching, Germany



Abstract

A wide variety of spectral features between 1 and $200\mu\text{m}$ have now been detected in Active Galactic Nuclei from the ground and with the ISO satellite. This rich spectrum is illustrated and its diagnostic value reviewed with particular emphasis on recent progress in detecting Broad Line Regions and the use of infrared 'coronal' lines to probe gas kinematics and the UV/soft x-ray spectra of obscured AGN.

1 Introduction

Infrared spectroscopy is a potentially powerful tool for studying Active Galactic Nuclei (AGN) due both to the wider range of diagnostic features available and the much lower dust extinction at these wavelengths compared to the visible. Until recently, its exploitation has been severely limited by the relatively poor sensitivity and small formats of infrared detectors and the restricted wavelength coverage available from the ground. The situation is now changing rapidly, however, thanks to the on-going evolution of groundbased infrared array detectors and the increasing availability of spectra over the range 2.5 - $200\mu\text{m}$ obtained with the ISO satellite [17,29,11,45] and the Kuiper Airborne Observatory [21]. Given the space restrictions of this review I cannot attempt to be comprehensive and have therefore elected to give a quick overview of the detected features and to discuss in more detail only the use of recombination lines to probe for visually obscured broad line regions (BLR) and the origin and application of the many high excitation 'coronal' lines discovered recently in the infrared. For greater completeness, however, it is worth noting here that infrared spectroscopy of recombination lines plus CO, SiI and other stellar photospheric absorption features is providing important information on the morphology, age and relationship of starburst to AGN activity [28,19,13,35,20]; that recent line imaging and models of [FeII] and H_2 emission suggests that these lines could be predominantly excited by nuclear outflow shocks and/or x-rays in AGN [5,43,50] and that even some of the PAH feature emission may be associated with AGN heated dust [42].

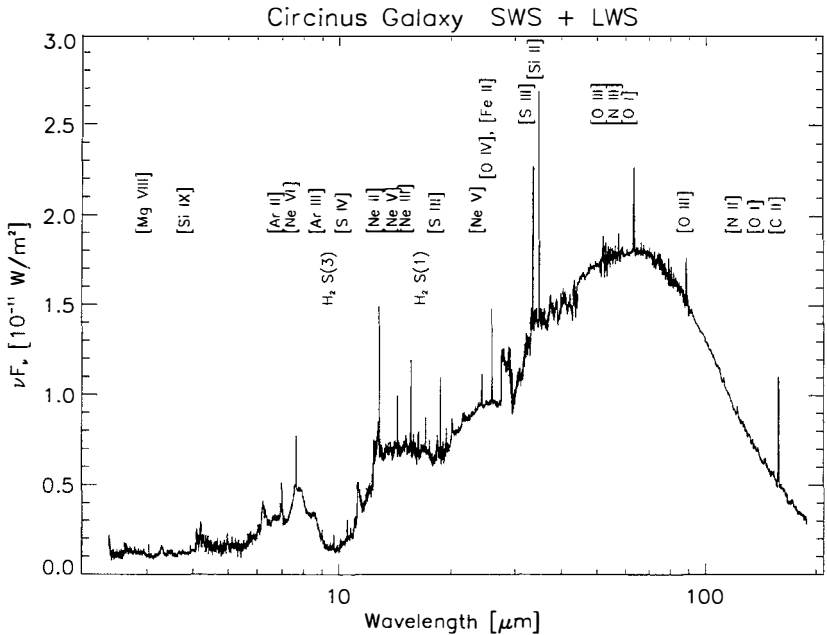


Figure 1: 2.5 - 200 μm spectrum of the Circinus galaxy obtained with the SWS [29] and LWS (unpublished) spectrometers on the ISO satellite.

2 Overview of AGN infrared diagnostic features

Near infrared (1-5 μm) spectra of AGN contain several well known H recombination ($\text{Pa}\alpha$, $\text{Pa}\beta$, $\text{Br}\gamma$..), $[\text{FeII}]$ and H_2 emission lines plus CO, SiI and other stellar absorption bands and a more recently discovered suite of prominent 'coronal' lines from species with ionization energies up to 400eV ($[\text{CaVIII}]$, $[\text{SiX}]$, $[\text{AlIX}]$, $[\text{SiVI}]$, $[\text{SiVII}]$, $[\text{SiIX}]$, $[\text{SiX}]$) [33,34,49,23]. Fig 1. shows an overlapping 2.5 - 200 μm spectrum of the Circinus galaxy obtained with the SWS (Short Wavelength) and the LWS (Long Wavelength) spectrometers on board the ISO satellite. This galaxy provides the closest (4 Mpc) example of a Seyfert 2 type nucleus surrounded by starburst activity and its spectrum has provided the first census of infrared spectral features over much of this wavelength range. The spectrum shows i) the far infrared continuum peak characteristic of 'infrared' galaxies ii) the 9.7 μm silicate absorption plus PAH emission features at 3.3, 6.6, 7.7, 8.6, 11.3 and 12.6 μm which dominate the mid-infrared region and which probably contain contributions from both AGN and starburst heated dust [42] iii) several H_2 vibration-rotation and rotational emission lines and iv) ionic fine structure lines from a wide range of elements and ionization energies. Fig. 2. is a plot of ionization energy versus wavelength for the infrared fine structure lines detected to date. Some of those in the ISO range which are not clearly visible in the full - scan spectra in Fig. 1 have been observed in deeper spectra centred on the specific lines [29].

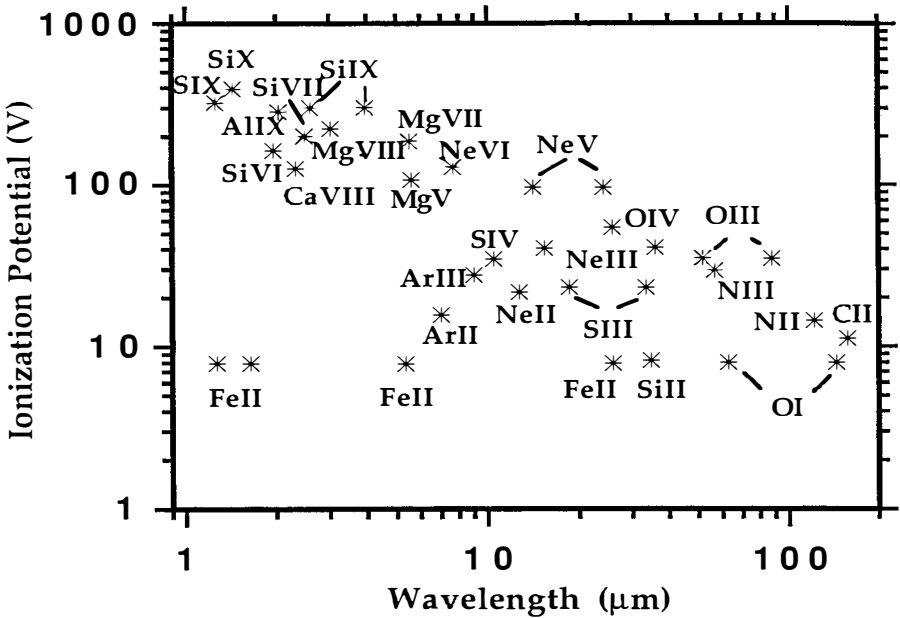


Figure 2: Ionization potential versus wavelength plot of infrared fine structure lines detected to date in AGN.

3 Infrared searches for AGN

Infrared hydrogen recombination line observations are providing important support to the unified Seyfert picture in which the BLR's in 'narrow line' objects are presumed to be obscured visually along the line of sight by a surrounding torus. A recent, extensive, survey involving observations of one or more of the $\text{Pa}\beta(1.28\mu\text{m})$, $\text{Br}\gamma(2.16\mu\text{m})$ and $\text{Br}\alpha(4.05\mu\text{m})$ lines in a sample of 33 Seyfert 2's [50] has confirmed earlier detections of broad lines in three cases [4,40] and added 6 possible new detections. Despite the relatively small number of detections and the fact that the observed linewidths are at the low end of the Seyfert 1 range this result is still significant because, although suffering lower extinction, the infrared lines are intrinsically fainter than the visible Balmer lines used for the visible classifications and their detection is probably limited to optical depths $A_v \leq 25$. The positive detections therefore may correspond to just the fraction of Seyfert 2's whose BLR can be observed through the lower extinction 'throat' of the torus while the more edge-on cases remain obscured in the near infrared. Observations of longer wavelength lines are obviously of interest and are planned with ISO.

Of particular interest is the potential of infrared spectroscopy to detect AGN activity in Ultraluminous Infrared Galaxies. Early searches for broad $\text{Br}\gamma$ and $[\text{SiVI}]$ coronal line emission in the K band window [15,25] as evidence for obscured AGN's proved negative. More recently, however, broad $\text{Pa}\alpha$ lines have been seen in 7 out of 10 ULIRG's classified optically as Seyfert 2's (of which 3 may also show $[\text{SiVI}]$) whereas 15 classified optically as LINERS or HII galaxies show no signs of an obscured BLR or $[\text{SiVI}]$ emission [51]. Preliminary analysis of ISO spectra of ULIRG's have also not so far revealed longer wavelength coronal lines [22] and

the [NeV](14.3 μ m)/[NeII](12.8 μ m) and [OIV](26)/[NeII] upper limits in Arp220 are about an order of magnitude lower than expected in comparison with known AGN even after correction for an extinction $A_v = 50$ derived from recombination line ratios [46]. Infrared spectroscopy is therefore already providing important support to both sides of the starburst versus AGN debate!

4 The coronal line region

4.1 Ionization mechanism

Within the context of AGN, the term coronal is usually applied to collisionally excited forbidden transitions between low lying states of highly ionized species. In the visible, [FeVII](0.6086 μ m; 99eV) was first detected by Seyfert [41] and [FeX](0.6374 μ m; 235eV), [FeXI](0.7892 μ m; 262eV), [FeXIV](0.5303 μ m; 361eV) have subsequently been found to be commonly present. Apart from the Fe lines, however, the only other visible coronal lines observed are [NeV](0.3425 μ m,97eV)[2] and [SVIII](0.9912 μ m; 281eV)[37]. Despite the long history of coronal line studies there remains a fundamental controversy as to whether they arise in hot ($\sim 10^6$ K) collisionally ionized gas as proposed initially by Oke & Sargent [31] or in gas photoionized by the AGN EUV continuum as first suggested by Osterbrock [36]. More recent variants include mixtures of photoionized and hot gas [52,53] and photoionization by radiative shocks [9,47]. The density and hence extent of the coronal line region also remains unclear with proposals ranging from 1 cm⁻³ [18] in the extended ISM to $\sim 10^{11}$ cm⁻³ [38] in the BLR which have proved difficult to test in the absence of high resolution spatial information and because models of the visible coronal lines are relatively insensitive to density because of their high critical densities (typically $\sim 10^{8-9}$ cm⁻³). Given this history, the recent observations of infrared coronal lines are clearly of considerable interest because they suffer lower extinction; provide more complete coverage of the ionization energy range and are emitted by a wider range of elements (S, Si, Mg, Ne and Ca) thus providing additional abundance information. The lines detected to date are [NeV](14.32 and 24.31 μ m; 97eV), [NeVI](7.66; 126); [MgV](5.62; 109), [MgVII](5.51; 187), [MgVIII](3.03; 225); [CaVIII](2.32; 127.7); [SiVI](1.96; 167), [SiVII](2.48; 205), [SiIX](3.94; 303), [SiX](1.43; 400); [AlIX](2.043; 285); [SiX](1.25; 328). Combining the earlier visible studies with more recent analyses of the infrared coronal lines leads to the following arguments for and against the various ionization mechanisms.

4.1.1 Photoionization. Photoionization by the AGN power law spectrum ($\sim \nu^{-1}$) appears to be the most widely accepted mechanism. Recent support has been added by models which reproduce the infrared line strengths to within a factor of a few which are within the uncertainties of the atomic parameters [44,29,30].

Photoionization by stars is expected to be negligible because their spectra fall off far too steeply in the EUV/soft x-ray range. A direct observational confirmation is provided by the high excitation planetary nebula NGC6302 whose [SiIX]/[SiVI] ratio is at least a factor 1000 smaller than observed in Seyferts despite a central star temperature ~ 380000 K [24,39].

Photoionization by fast (400 km s⁻¹), radiative, shocks associated with mass outflow from the nucleus has been proposed as a general alternative to direct photoionization by the AGN [9,47]. A detailed model for NGC1068 [8] fits the observed NLR fluxes within a factor ~ 2 but does not generate coronal [FeX]. Based on tabulated ionic column densities in the photoionized pre-cursor [9] it appears that this problem also extends to the infrared coronal lines. Even at the highest shock velocity of 500 km s⁻¹ for example, the [SiIX]/[SiVI] and [SiX]/[SiVI] ratios are too small by ~ 50 and 400 respectively [30].

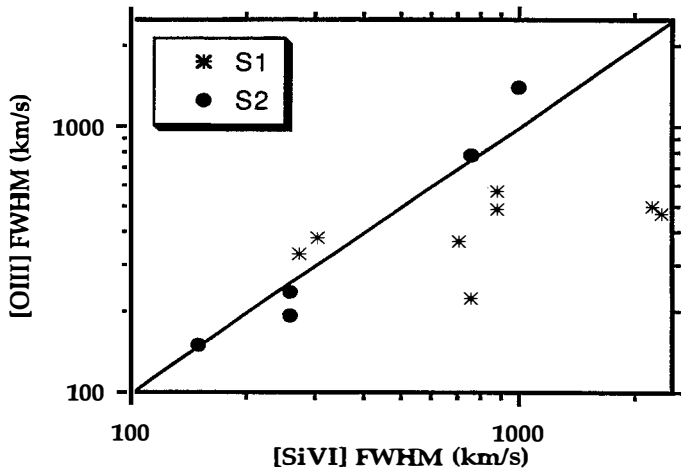


Figure 3: Plot of visible [OIII] versus infrared [SiVI] FWHM for Seyfert types 1 and 2 galaxies. Visible data are from [1,10,57] and infrared from [25,14]

4.1.2 Collisional ionization. Collisional ionization in hot ($\sim 10^6\text{K}$) gas appears to be excluded as a general explanation by - i) [FeVII] line ratios which indicate gas temperatures $\sim 20000\text{ K}$ [6,12,54] ii) the linewidths in some cases (e.g. $\leq 150\text{ km s}^{-1}$ in Circinus) which are narrower than expected in shock heated gas [52] iii) lack of similarity between Seyfert and SNR spectra [32] iv) the observed [Fe]/[Si] and [Fe]/[S] line ratios which are considerably lower than expected in hot gas models due to enhancement of the [Fe] lines by electron collisions of their high lying states [34,24] and the large masses of gas which would have to be shocked to account for the line luminosities ($\simeq 600\text{ M}_\odot/\text{yr}$ in NGC1068 [32]). Nevertheless, evidence for higher temperature ($\sim 10^5\text{K}$) gas [54] and models predicting an enhancement of high excitation lines for SN exploding in very high density gas [47] means that possible contributions from shocked gas cannot be excluded in all cases.

4.2 Kinematics, location and extent of the CLR

Visible emission lines in Seyfert spectra tend to exhibit blueshifts relative to the systemic velocity and linewidths which both increase with ionization energy and critical density. These characteristics are consistent with a decelerating outflow (or inflow but less likely); radially decreasing ionizing degree and density and higher dust extinction towards the receding gas. For the coronal lines specifically these characteristics suggest an origin primarily in an interface region between the BLR and NLR. However, although statistically significant within the samples observed, some individual Seyferts - particularly type 2's - show no or even the opposite trends [1]. Because of the role of extinction in causing the blueshifts of the visible lines it was to be expected that infrared coronal lines would exhibit smaller blueshifts and possibly broader lines or double peaked profiles produced by bi-polar outflows. The two best studied Seyferts in the infrared to date are the Circinus galaxy [34] and NGC1068 [24] - both officially type 2's. In Circinus, all the observed emission lines in the visible and infrared are extremely narrow $\leq 150\text{ km s}^{-1}$ and exhibit no dependence on ionization energy or critical density; blueshifts are small $\leq 40\text{ km s}^{-1}$ and not significantly different between the visible and infrared. In NGC1068 both

the visible and infrared coronal lines exhibit the same large (300km s^{-1}) blueshift relative to the systemic velocity and the FWHM of [SiIX]($3.94\mu\text{m}$, 303eV) is comparable or slightly narrower than visible lines formed in the NLR. In both cases the results are consistent with outflow within the single sided ionization cones seen in the visible i.e red-shifted counter flows either don't exist or the extinction to them is too high for their detection even at relatively long infrared wavelengths. In NGC1068, whose cone is inclined at $\simeq 80^\circ$ to the line of sight [7], the projected velocity of 300km s^{-1} corresponds to an outflow velocity of $\sim 1500\text{km s}^{-1}$. Higher observed velocities could therefore be expected in type 1 Seyferts whose outflows should be observed more pole on according to the current unified Seyfert model. Statistical studies in the infrared are limited to the following relatively small samples observed in the [SiVI]($1.963\mu\text{m}$, 167eV) line - the Seyfert 1's IC4329A, Tol 0108-383, NGC3516, NGC3783, NGC4051, NGC4151, NGC5548, Mkn509 [25,14] and the Seyfert 2's Mkn463, NGC4507, NGC5506, Circinus and NGC1068 [25]. The largest blueshift is the 300km s^{-1} in NGC1068 followed by 200km s^{-1} in NGC5548 and the remainder are consistent with 0 within the uncertainties although it is interesting that both [SiVI] and the visible [FeX] lines in NGC4507 appear to be red-shifted by $\sim 100\text{km}^{-1}$ [25,1]. With two exceptions [14], the velocity FWHM are $< 1000\text{km s}^{-1}$ which, combined with the small shifts, implies that high velocity flows as inferred in NGC1068 are not common in Seyferts. In most cases where suitable visible data are available the [SiVI] line is comparable to or broader than [FeX] - consistent with the infrared line probing closer to the nucleus. Greater systematic differences are seen when comparing the [SiVI] linewidths with those of [OIII]($0.5007\mu\text{m}$) in the NLR as shown in Fig.3. In the case of Seyfert 2's, the linewidths are comparable suggesting that [SiVI] arises predominantly in the NLR. In Seyfert 1's, however, [SiVI] exhibits a much larger range in width and becomes increasingly broader than the [OIII] line as its width increases suggestive of coronal line contributions from the BLR. The two cases showing $\text{FWHM} > 2000\text{km}^{-1}$, approaching those of the permitted H line widths, are NGC3516 and Mkn509 for which this explanation was proposed in the discovery paper [14]. In Cygnus A, an AGN powered radio galaxy, [SiVI] is also much broader ($\simeq 1200\text{km s}^{-1}$) than [FeX]($\simeq 700\text{km s}^{-1}$) and the lower excitation NLR lines ($\simeq 400\text{-}500\text{km s}^{-1}$)[56].

Although direct spatial information on the coronal line emitting region is scarce, line images of both Circinus and NGC1068 show that it is elongated in the direction of the ionization cones defined by [OIII] and that its extent from the nucleus increases with decreasing ionization energy. In Circinus [SiVI](167eV) extends $\simeq 40\text{pc}$ (c.f. $\sim 500\text{pc}$ for [OIII]); [AlIX](285eV) $< 20\text{pc}$ [23] and [FeXI](262eV) $< 10\text{pc}$ [34]. In NGC1068 the [SiVI] emission extends over $\simeq 200\text{pc}$ with a peak $\simeq 50\text{pc}$ from the nucleus along the axis of the ionization cone [48],[24] and [FeX](235eV) appears to be confined within a region $< 20\text{pc}$ [24] whereas the lower excitation [FeVII] and [NeV] lines are seen far out in the cone. Extended, bi-polar [FeVII] emission is also observed in the Seyfert 1 galaxy NGC3516 [16].

In summary, therefore, the new infrared data tends to add to and support the picture in which the coronal lines extend from the BLR out into the NLR with decreasing ionization energy and indicate that any BLR component in the Seyfert 2's is obscured even in the near infrared - which is not surprising given the difficulty of detecting broad Br γ components.

5 Shape of the AGN UV and X-ray continuum

Under the assumption that coronal lines do predominately arise in gas photoionization by the AGN their strengths provide a diagnostic tool for determining the spectral shape of the ionizing continuum. The coronal lines are of particular interest because they probe the EUV/soft x-ray region. Including lower excitation lines is also important, however, to test for the presence of

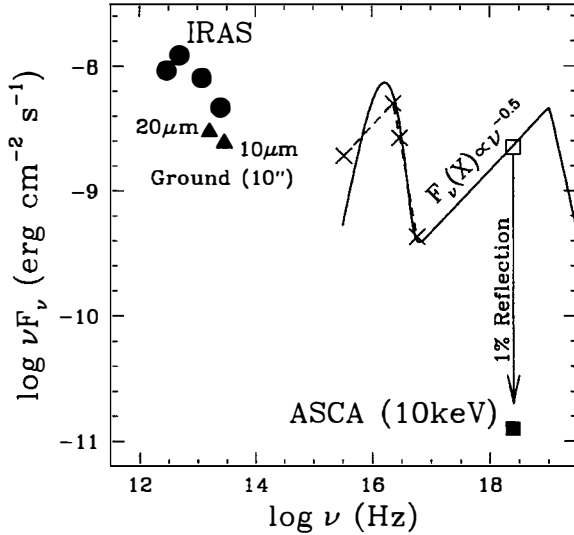


Figure 4: Intrinsic EUV/soft x-ray spectrum of the Circinus nucleus, derived from photoionization modelling, together with infrared continuum and x-ray observations [29].

the UV bump or break inferred from observations of Seyfert 1 galaxies and quasars [55] but the usefulness of lines with ionization energies $\leq 40\text{eV}$ is increasingly limited due to contamination by starburst activity. The most detailed study of this type to date is that made of the Circinus galaxy [29] for which a large body of high quality visible, groundbased infrared and ISO spectra are now available as discussed and partly illustrated already. This galaxy provides an excellent laboratory for studying the AGN phenomenon due to its proximity (4 Mpc) and prominent ionization cone containing a well defined high excitation knot which provides additional information on the ionization rate and UV continuum of the central ionizing source [26]. Constraints applied to the photoionization modelling were i) $L_{\gamma} = 10^{53.3}$ photons s^{-1} deduced from $\text{H}\alpha$ in the high excitation knot assuming an intrinsically isotropic source ii) covering factor of 0.05 deduced from the nuclear $\text{Br}\alpha$ flux and ionization rate iii) $n_e = 5000\text{cm}^{-3}$ from $[\text{NeV}]14.3/24.3\mu\text{m}$ and iv) solar abundances. The derived UV/x-ray photoionization spectrum fits the large number of emission lines in the range 50-330eV to an absolute accuracy $\simeq 2$ (better would be suspicious given uncertainties in the collision strengths) and is shown in Fig.4. together with the observed infrared and x-ray continua. Its main features are the hard EUV/x-ray power-law component and the pronounced 'bump' around 70eV which can equally well be represented by a broken power law within the observational constraints. As with all such photoionization models the result shown cannot be claimed to be unique. For example, equally good fits appear to be possible assuming a single power law (although somewhat steeper) and a mix of radiation and matter bounded clouds [3]. With the approach adopted here, however, the spectrum obtained matches those deduced from interpolating UV and x-ray continuum observations of Seyfert 1's

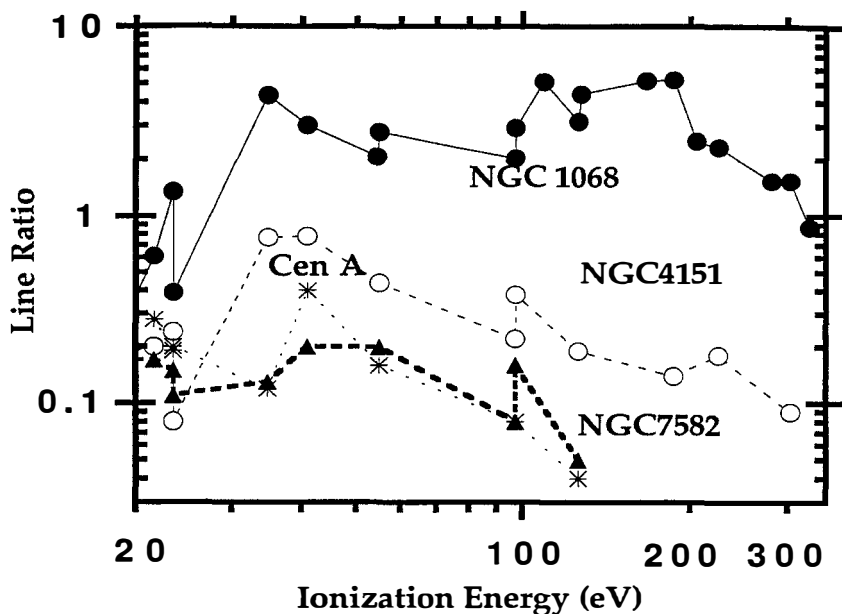


Figure 5: Infrared line strengths relative to the Circinus galaxy versus ionization energy for different types of AGN.

and quasars with the IUE, ROSAT and Ginga satellites [55]. The power law component is also consistent with the x-ray spectrum at higher energies and its absolute flux at 10keV with the canonical value of 1% for the reflection of the x-ray mirror [27]. The total intrinsic UV/x-ray luminosity is also sufficient to account for most of the infrared luminosity via dust heating. Lacking information on the detailed cloud structure, therefore, this model suggest that the intrinsic AGN spectrum in this Seyfert 2 galaxy is similar to those in Seyfert 1's.

The 'Circinus model' also provides a good fit to the emission line spectrum of NGC1068 except that its EUV spectrum is probably somewhat steeper[30]. Infrared spectra of NGC4151 (Seyfert 1), NGC7582 (NLX) and CenA (AGN powered radio galaxy) are also similar except for the systematic and more pronounced decrease in line intensity relative to Circinus as a function of ionization energy which is clearly evident in Fig. 5. Although detailed modelling has yet to be performed, therefore, it is likely that similar photoionization models but with even steeper EUV spectra will apply. It is curious that the Seyfert 2's appear to have the hardest ionizing spectra but too early to draw any conclusion concerning a systematic difference amongst AGN types given the small size of the sample.

Acknowledgements. During the preparation of this review I have benefitted greatly from discussions with my collaborators E. Oliva in Florence and D. Lutz, E. Sturm and R. Genzel at the MPIE in Garching and am grateful to the latter for permission to include the long wavelength part of the Circinus spectrum and some of the SWS data used to construct Fig. 5 prior to publication.

References

- [1] Appenzeller, I., & Ostriker, R. 1988, *AJ*, 95, 45
- [2] Bergeron, J., Petitjean, P., & Durret, F. 1989, *A&A*, 213, 61
- [3] Binette, L., Wilson, A.S., Raga, A., & Storchi-Bergmann, T. 1997, *A&A* (submitted)
- [4] Blanco, P.R., Ward, M.J., & Wright, G.S. 1990, *MNRAS*, 242, 4P
- [5] Blietz, M., Cameron, M., Drapatz, S., Genzel, R., Krabbe, A., van der Werf, P.P., Sternberg, A., & Ward, M. 1994, *ApJ*, 421, 92
- [6] Bokkenberg, A. *et al.* 1975, *MNRAS*, 173, 381
- [7] Cecil, G., Bland, J. & Tully, R. B. 1990. *ApJ*, 355, 70
- [8] Dopita, M. A. 1997, to appear in *Proceedings of the Ringberg Workshop on NGC1068* (J. Gallimore & L. Tacconi eds.), *Astrophys. Sp. Sci.* (in press).
- [9] Dopita, M. A. & Sutherland, R. S. 1996, *ApJS*, 102, 161
- [10] Feldman, F.R., Weedman, D.W., Balzano, V.A., & Ramsey, L.W. 1982, *ApJ*, 256, 427
- [11] Fischer, J., *et al.* these proceedings
- [12] Fosbury, R. A. E. & Sansom, A. E. 1983, *MNRAS*, 204, 1231
- [13] Genzel, R., Weitzel, L., Tacconi-Garman, L.E., Blietz, M., Cameron, M., Krabbe, A., Lutz, D., Sternberg, A. 1995, *ApJ*, 444, 129
- [14] Giannuzzo, E., Rieke, G.H., & Rieke, M.J. 1995, *ApJ*, 446, L5
- [15] Goldader, J.D., Joseph, R.D., Doyen, R., & Sanders, D.B. 1995, *ApJ*, 444, 97
- [16] Golev, V., Yankulova, I., Bonev, T., & Jockers, K. 1994, *ApL*, 29, 239
- [17] Kessler, M.F. *et al.* 1996, *A&A*, 315, L27
- [18] Korista, K. T. & Ferland, G.J. 1989, *ApJ*, 343, 678
- [19] Krabbe, A. 1997, in B. M. Peterson, F.-Z. Cheng & A.S. Wilson (eds), *IAU Colloq. 159, Emission Lines in Active Galaxies: New Methods and Techniques* (ASP: San Francisco), ASP Conf. Series 113, 325
- [20] Kroker, H., Genzel, R., Krabbe, A., Tacconi-Garman, L.E., Tecza, M., Thatte, N., & Beckwith, S.V.W. 1996, *ApJ*, 463, 55
- [21] Lord, S.D. *et al.* 1995, *Airborne Astronomy Symposium on the Galactic Ecosystem: From Gas to Stars to Dust*. ASP 73, 151
- [22] Lutz, D. *et al.* 1996, *A&A*, 315, L137
- [23] Maiolino, R., Thatte, N., Kroker, H., Gallimore, J.F., & Genzel, R. 1997, in B. M. Peterson, F.-Z. Cheng & A.S. Wilson (eds), *IAU Colloq. 159, Emission Lines in Active Galaxies: New Methods and Techniques* (ASP: San Francisco), ASP Conf. Series 113, 351
- [24] Marconi, A., van der Werf, P.P., Moorwood, A.F.M., Oliva, E. 1996, *A&A*, 315, 335
- [25] Marconi, A., Moorwood, A.F.M., Salvati, M. & Oliva, E. 1994, *A&A*, 291, 18
- [26] Marconi, A., Moorwood, A.F.M., Origlia, L. & Oliva, E. 1994, *The Messenger*, 28, 20
- [27] Matt, G. *et al.* 1996, *MNRAS*, 281, 69
- [28] Moorwood, A.F.M. 1996, *Space Science Reviews*, 77, 303
- [29] Moorwood, A.F.M. *et al.* 1996, *A&A*, 315, L109
- [30] Moorwood, A.F.M., Marconi, A., van der Werf, P.P., & Oliva, E., 1997, to appear in *Proceedings of the Ringberg Workshop on NGC1068* (J. Gallimore & L. Tacconi eds.), *Astrophys. Sp. Sci.* (in press).
- [31] Oke, J. B., & Sargent, W. L. W. 1968, *ApJ*, 151, 807

- [32] Oliva, E. 1997, in B. M. Peterson, F.-Z. Cheng & A.S. Wilson (eds), *IAU Colloq. 159, Emission Lines in Active Galaxies: New Methods and Techniques* (ASP: San Fransico), ASP Conf. Series 113, 288
- [33] Oliva, E. & Moorwood, A.F.M. 1990, *ApJL*, 348, L5
- [34] Oliva, E., Salvati, M., Moorwood, A.F.M. & Marconi, A. 1994, 288, 457
- [35] Oliva, E., Origlia, L., Kotilainen, J.K., & Moorwood, A.F.M. 1995, *A&A*, 301, 55
- [36] Osterbrock, D.E. 1969, *Ap. Letters*, 4, 57
- [37] Osterbrock, D. E., & Fulbright, J. P. 1996, *PASP*, 108, 183
- [38] Penston, M. V., Fosbury, R.A.E., Boksenberg, A., Ward, M.J., & Wilson, A.S. 1984, *MNRAS*, 208, 347
- [39] Pottasch, S. *et al.* 1996, *A&A*, 315, L261
- [40] Rix, H.-W., Carleton, N.P., Rieke, G., & Rieke, M. 1990, *ApJ*, 364, 77
- [41] Seyfert, C. K. 1943, *ApJ*, 97, 28
- [42] Siebenmorgen, R., Moorwood, A.F.M., Freudling, W., & Käufel, H.-U. 1997, *A&A* (in press)
- [43] Simpson, C., Forbes, D., Baker, A. C., & Ward, M.J. 1996, *MNRAS*, 283, 777
- [44] Spinoglio, L. & Malkan, M. A. 1992, *ApJ*, 399, 504
- [45] Spinoglio, L. these proceedings
- [46] Sturm, E. *et al.* 1996, *A&A*, 315, L133
- [47] Terlevich, R., Tenorio-Tagle, G., Franco, J. & Melnick, J. 1992, *MNRAS*, 255, 713
- [48] Thatte, N., *et al.* 1996, in D. Minnitti & H.-W. Rix (eds), *Spiral Galaxies in the Near-IR. ESO Astrophysics Symposia* (Springer-Verlag), 333
- [49] Thompson, R. I. 1996, *ApJL*, 459, L61
- [50] Veilleux, S., Goodrich, R.W. & Hill, G. J. 1997, *ApJ*, 477, 631
- [51] Veilleux, S., Sanders, D.B., & Kim, D.-C. 1997, *ApJ* (in press, July)
- [52] Viegas-Aldrovandi, S.M. & Contini, M. 1989, *A&A*, 215, 253
- [53] Viegas, S.M., & Contini, M., 1997, in B. M. Peterson, F.-Z. Cheng & A.S. Wilson (eds), *IAU Colloq. 159, Emission Lines in Active Galaxies: New Methods and Techniques* (ASP: San Fransico), ASP Conf. Series 113, 365
- [54] Wagner, S.J. 1997, in B. M. Peterson, F.-Z. Cheng & A.S. Wilson (eds), *IAU Colloq. 159, Emission Lines in Active Galaxies: New Methods and Techniques* (ASP: San Fransico), ASP Conf. Series 113, 298
- [55] Walter, R., Orr, A., Courvoisier, T.J.-L., Fink, H. H., Makino, F., Otani, C., & Wamsteker, W. 1994, *A&A*, 285, 119
- [56] Ward, M.J., Blanco, P.R., Wilson, A.S., & Nishida, M. 1991, *ApJ*, 382, 115
- [57] Whittle, M. 1985, *MNRAS*, 216, 817